View Article Online / Journal Homepage / Table of Contents for this issue

PAPER

NJC
www.rsc.org/njc

Colorimetric detection of chemical warfare simulants†

Karl J. Wallace,[a] Jeroni Morey,*[b] Vincent M. Lynch[a] and Eric V. Anslyn*[a]

[a] *Department of Chemistry and Biochemistry, The University of Texas at Austin, 24th and Speedway, Welch 5.201, Austin, TX 78712-1167, USA. E-mail: anslyn@ccwf.cc.utexas.edu; Fax: +1 (512) 471 7791; Tel: +1 (512) 471 0068*

[b] *Departament de Química, Universitat de les Illes Balears, 07122 Palma de Mallorca, Spain. E-mail: jeroni.morey@uib.es*

Received (in St Louis, MO, USA) 3rd May 2005, Accepted 31st August 2005
First published as an Advance Article on the web 22nd September 2005

Downloaded by University of California - Los Angeles on 01 January 2013
Published on 22 September 2005 on http://pubs.rsc.org | doi:10.1039/B506100H

Two simple chromogenic indicators (**4**) and (**5**), containing different supernucleophilic moieties, have been synthesized. Upon phosphorylation with two chemical warfare agent (CWA) simulants, a hypsochromic shift of approximately 50 nm is observed in an NaOH–DMSO solution. The oximate supernucleophile was found to be a better supernucleophile than the hydrazone moiety. Two X-ray crystal structures were obtained from unexpected synthetic side products obtained in this study. These will also be discussed.

Introduction

It is well established that many organophosphorus compounds are powerful neurotoxic agents that inhibit acetylcholinesterase (AchE) by the process of phosphorylation.[1,2] A particularly dangerous class of organophosphorus compounds are the phosphoryl fluoride containing species. Two such species are the Chemical Warfare Agents (CWAs) sarin (isopropyl methylphosphonofluoridate), and soman (pinacolyl methylphosphonofluoridate), referred to as GB and GD agents, respectively. There has been significant interest in the decontamination[3,4] and detection[5–7] of CWAs over the last five decades. One approach uses chromogenic detector reagents, which directly bind to, or react with, a target nerve agent, causing a modulation in the UV-Vis wavelength.[8–10]

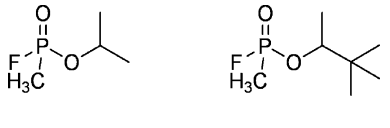

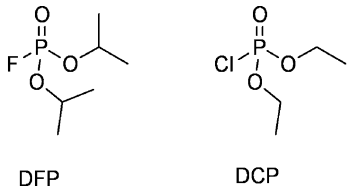

One common CWA simulant is diisopropyl fluorophosphate (DFP). A less toxic simulant that is also often used is diethyl chlorophosphate (DCP). Recently, Swager introduced a fluorescent indicator that undergoes a dramatic spectral change in response to the cyclization of a flexible chromophore. A rigid and highly conjugated fluorophore is created on the addition of DFP, causing an 'off–on' response in the micromolar concentration range.[6] Yet, the system uses an alcohol as a nucleophile, and hence the rate of reaction with DFP (let alone that anticipated with sarin/soman) is quite slow (half-life approaching one hour).

Herein, we report the development of two simple organic molecules as indicators for phospho-fluorides: an oxime (**4**) and a hydrazone (**5**).

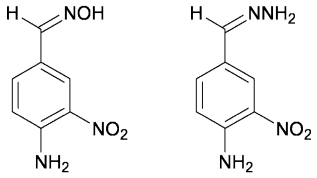

4 **5**

Results and discussion

Design criteria

Our approach was to create a very simple colorimetric system that contains a highly nucleophilic moiety, known as a supernucleophile. A supernucleophile is a reactive species whereby an atom containing an unshared electron pair, typically a nitrogen or oxygen atom, is adjacent to the nucleophilic center. This increases the nucleophilicity of the reactive center, a phenomena commonly known as the α-effect.[11] Two such supernucleophiles are oximate (RNO^-) functionalities and hydrazone ($RNNH_2$) moieties. Both the oximate and hydrazone reactive sites can react with the phosphorus(v) center of the CWA simulant. For the molecule to act as a colorimetric system, a UV-Vis absorbance spectral change needs to be observed. A typical functional group that is an ideal UV-Vis 'handle' is the nitro moiety.

Synthesis

Commercially available 4-acetamidobenzaldehyde was reacted with fuming nitric acid (>90%). The nitro group is introduced into the *meta* position in relation to the aldehyde functionality and the *ortho* position in relation to the amide group of the benzene ring, forming 4-acetamido-3-nitrobenzaldehyde (**2**) in moderate yield, typically 50%. The inclusion of the nitro group

† Electronic supplementary information (ESI) available: UV-Vis spectra of **5**. See http://dx.doi.org/10.1039/b506100h

DOI: 10.1039/b506100h

View Article Online

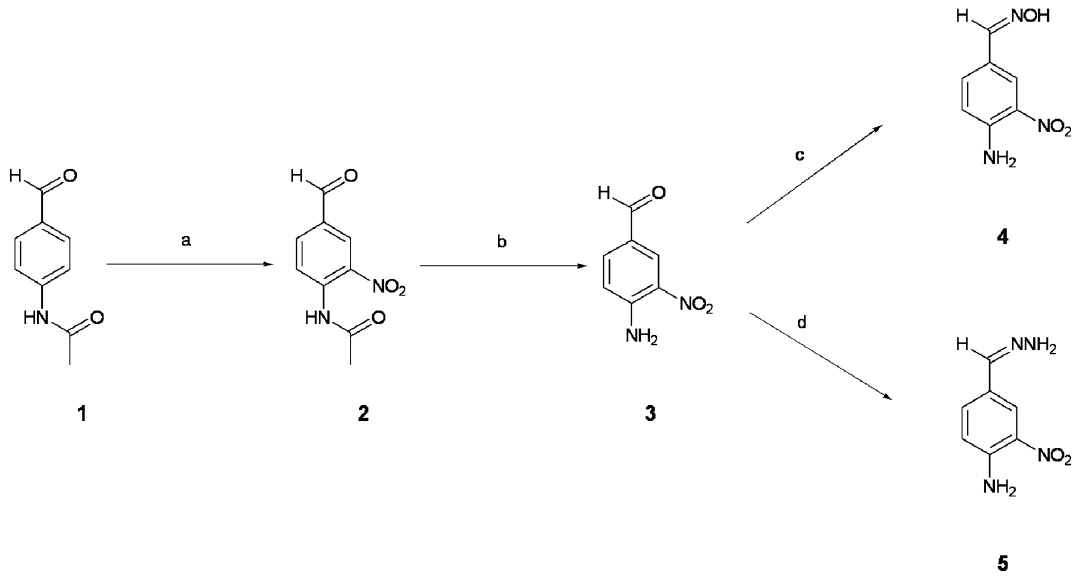

Scheme 1 The preparation of 4-amino-3-nitrobenzaldoxime (**4**) and 4-hydrazonomethyl-2-nitrophenylamine (**5**): (a) fuming HNO_3 (>90%); (b) HCl; (c) $NH_2OH \cdot HCl$, NaOH; (d) $H_2NNH_2 \cdot H_2O$, cat *p*-TsOH.

Published on 22 September 2005 on http://pubs.rsc.org | doi:10.1039/B506100H
Downloaded by University of California - Los Angeles on 01 January 2013

is clearly apparent in the appearance of the NO_2 symmetric and antisymmetric stretches at 1458 and 1377 cm^{-1}, respectively, in the IR spectrum. Addition of hydrochloric acid to **2** subsequently produces 4-amino-3-nitrobenzaldehyde (**3**) in 75% yield. Compound **3** is converted to the oxime **4** by reacting **3** with hydroxylamine hydrochloride and sodium hydroxide. Compound **3** was also treated with hydrazine hydrate, with a catalytic amount of *p*-toluenesulfonic acid, to produce 4-hydrazonomethyl-2-nitrophenylamine (**5**), Scheme 1.[12] All compounds were fully characterized using ^1H and ^{13}C NMR, HRMS, IR and UV-Vis spectroscopy, which are in agreement with the proposed structures.

Solution studies

Due to the high toxicity of CWAs sarin and soman, model compounds DCP and DFP were used in this study. However, phosphoryl–chloride bonds are significantly weaker than phosphoryl–fluoride bonds (326 and 490 kJ mol^{-1}, respectively), and therefore a direct comparison of DCP with CWA must take these bond strengths into consideration. In solution, it is well documented that DFP and DCP are unstable to basic medium over a prolonged period of time. The Sigma-Aldrich company states that the half-life of DFP at pH = 7.5 is only one hour; therefore, all samples were prepared as fresh solutions, before each study.

A base is required to deprotonate the oxime functionality to form the oximate anion. A set of ^1H NMR and mass spectroscopy experiments where carried out to determine whether or not **4** is susceptible to nucleophilic attack by the phosphorus(v) center. A sample of **4** was prepared by dissolving **4** in a 1 : 1 mixture of (DMSO-d_6)–(D_2O–NaOH, 1 mol dm^{-3}) solution in an NMR tube and the ^1H NMR spectrum was recorded. Three signals appear at δ 7.05, 7.75 and 8.08 ppm, assigned to the aromatic protons on the benzene core of **4**. Upon addition of 1.1 equivalents of DCP, three new sets of signals immediately appeared in a more downfield region of the NMR spectrum and were assigned to the oximate–DCP complex. The signals assigned to the ethyl protons in DCP appear at δ 1.47 and 3.30 ppm, and on the addition of the oximate, two sets of new signals appear at δ 1.11 and 3.84 ppm. The sample tube was left to stand for 24 h and the ^1H NMR spectrum was recorded again. A third set of aromatic signals appeared in the spectrum at δ 8.44, 7.32 and 6.96 ppm. The mass spectrum of the NMR sample clearly showed the existence of three components. The appearance of the third set of signals after 24 h suggested that, over time, the oximate–DCP complex is unstable. It is well documented that keto-oximes undergo a Beckmann rearrangement to form secondary amides. However, aldo-oximes have been shown to undergo dehydration to form nitrile species. In this particular example, 4-amino-3-nitrobenzonitrile (**6**), was evident as a minor product, from the ^1H NMR spectra and the $[M]^+$ peak observed at 163 in the mass spectra, Scheme 2.[13]

Further evidence to support the existence of the oxime–DXP adduct was seen in the ^{31}P NMR spectra. A DCP solution of DMSO-d_6 and D_2O–NaOH was prepared and the ^{31}P NMR spectrum recorded (δ_P = 0.64 ppm). On addition of 1 equivalent of oxime **4** the phosphorus signal shifted to δ_P = 1.82 ppm; the same trend is also observed for DFP.

UV-Vis studies

Experiments were carried out by titrating aliquots of DCP and DFP into a solution of **4**, (3×10^{-4} mol dm^{-3} in a 1 : 1 mixture of DMSO–NaOH at room temperature). In both cases, the initial UV-Vis spectra showed a broad band at λ_{max} = 461 nm,

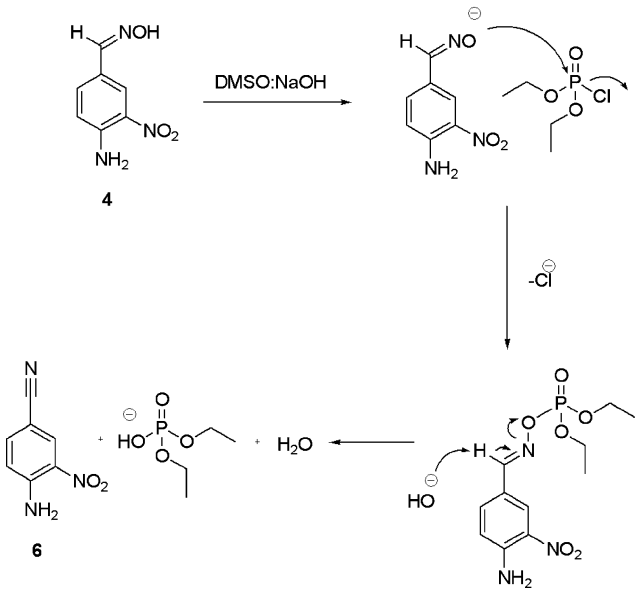

Scheme 2 Proposed mechanism for the nucleophilic attack of **4** undergoing dehydration to form 4-amino-3-nitrobenzonitrile (**6**).

View Article Online

Downloaded by University of California - Los Angeles on 01 January 2013
Published on 22 September 2005 on http://pubs.rsc.org | doi:10.1039/B506100H

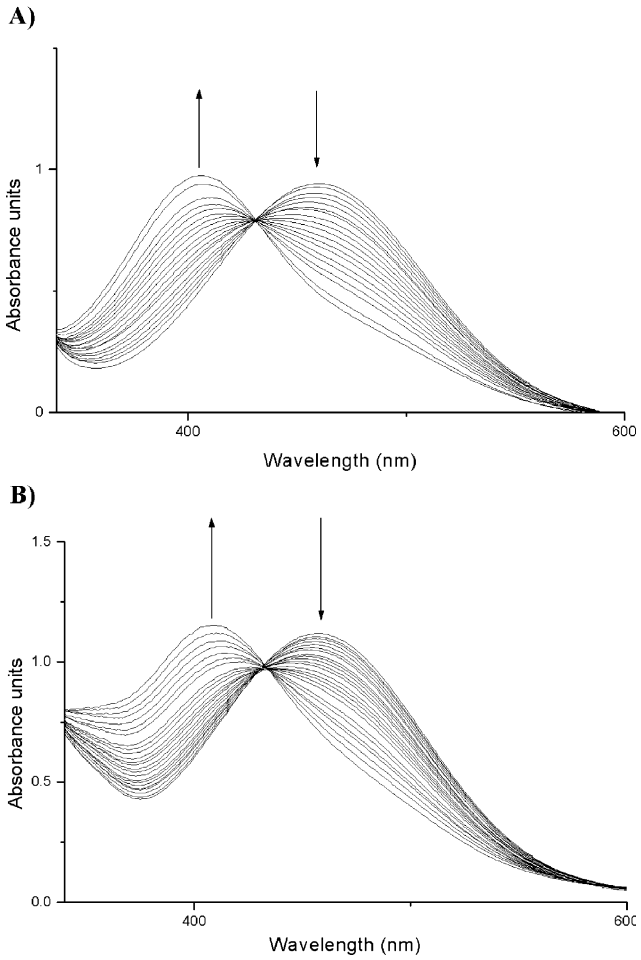

Fig. 1 The UV-Vis titration spectra of **4** upon addition of DCP (top) and DFP (bottom) in NaOH–DMSO solution (3×10^{-4} mol dm^{-3}).

assigned to the n–π^* transition.[14] Upon the gradual addition of DCP, the absorbance intensity at 461 nm decreased with the appearance of another band hypsochromically shifted to 410 nm through an isosbestic point, 431 nm, Fig. 1. The same trend is observed with the addition of aliquots of DFP to **4**. Here a decrease in absorbance intensity at 461 nm is accompanied by another band increasing at 413 nm through an isosbestic point at 437 nm.

It is well known that strong bases such as NaOH can react with DFP, to form the less toxic hydrolysis product.[3] To confirm the result proposed in Scheme 2, a stronger but a far less nucleophilic base was used. A nitrogen–phosphorous super-base was chosen. The phosphazene base P$_4$-*t*Bu solution ($^{DMSO}pK_{BH} + = 30.25$) is approximately two orders of magnitude stronger than DBU ($^{MeCN}pK_{BH} + = 24.3$) but less nucleophilic. On the addition of the P$_4$ base to a solution of the oxime **4**, an intense band at 530 nm is observed. On addition of DFP the band is again hypsochromically shifted to 417 nm, analogous to the NaOH experiment. This is consistent evidence that the oxime supernucleophile is phosphorylating the DFP.

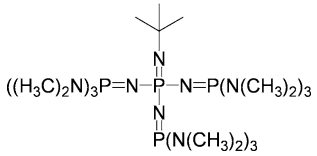

P$_4$-*t*-Bu phosphazene base

In 1970 Klopman tabulated data showing relative rate constants of various supernucleophiles with different substrates.[11] A hydrazone moiety was tabulated to be more nucleophilic than a simple oximate anion when treated with the same substrate. Therefore, it was anticipated that hydrazone **5** would react with the simulants in the same fashion (eliminating the use of NaOH) at the nucleophilic site.

Solutions of **5** were prepared in $CHCl_3$, MeOH, and DMSO, with the λ_{max} values at 425 nm, 432 nm and 461 nm, respectively. On addition of DFP a broad absorbance at λ_{max} at 353 nm grows in over time. However, the new species was identified as the protonated form of **5** and not the hydrazone–DFP adduct. This was due to a small amount of acid in the DFP solution and solvent (as $CHCl_3$ contains small traces of HCl). Protonation of compound **5** was confirmed by preparing a 1.5×10^{-4} mol dm^{-3} solution in MeOH to which 1 μL of 2 M HCl was added to the UV cell. This spectrum confirmed the appearance of the band at 350 nm, (see ESI†). The acidity problem was overcome by preparing a buffered solution of *p*-toluenesulfonic acid and Hünigs base 5.0×10^{-4} mol dm^{-3} in DMSO. The initial pH was recorded at 9.95 and the λ_{max} is at 445 nm for **5**. On the addition of 50 equivalents of DFP, an insignificant shift of 5 nm is observed in the blue direction and the final pH was recorded at 9.63. This small shift is attributed to the small change in concentration on the addition of DFP. It is interesting to note that **5** does not react with DFP in basic solution but **4**, when fully deprotonated reacts with the simulants. This is the opposite of the findings by Klopman, suggesting that **4** is a better supernucleophile than **5** under the conditions employed and with the substrates used herein.

Solid-state studies

It has been demonstrated that the oxime (**4**) can undergo phosphorylation with excess base in solution to form the oximate anion. An attempt was made to isolate the oximate salt by treating **4** with tetrabutylammonium hydroxide in a 1 mol dm^{-1} methanol solution. Unfortunately, the ^{1}H NMR spectrum of the isolated solid did not agree with the proposed structure. The integration of the aromatic signals was found to be half that of the CH_2 groups in the tetrabutylammonium cation, suggesting the formation of a dimer (**7**), and not the proposed oximate salt. This was confirmed by single crystal X-ray crystallography. Tetrabutylammonium hydroxide is probably deprotonating the oxime in solution. However, it is interesting to note that the isolated product is identified as the oximate–oxime dimer. It is unclear whether the excess of tetrabutylammonium hydroxide leads to only half the oxime molecules being deprotonated or if a proton is "picked" up during the recrystallization that subsequently forms the more stable oximate–oxime dimer.

X-Ray crystal structure of oxime–oximate dimer (7)

Crystals of compound **7** were grown by slow diffusion of diethyl ether into DMSO to form long orange needles, Fig. 2a. The oximate–oxime dimer observed in the solid-state is consistent with the ^{1}H NMR spectrum obtained for **7** in DMSO-d_6 solution. Oximate–oxime dimers are common in the literature and have been extensively studied by Maurin.[15–17] Interestingly, the intermolecular hydrogen bond lengths observed in **7** between O(3′)···O(3) are shorter than the typical intermolecular hydrogen bond length found in Maurin's system, presumably due to the electron withdrawing ability of the nitro group making the O(3′) hydrogen more acidic, thereby forming a stronger hydrogen bond with an oxime molecule. The crystal packing is dominated by the extensive hydrogen bonding network, which forms linear polymeric chains, Fig. 3a, with a combination of strong intramolecular hydrogen bonds [O(2)···HN(2) and N(1′)···HN(2′) 2.654(3) and 2.658(3)], and weaker intermolecular hydrogen bonds, [O(1′)···N(2) 4.202(3) and N(2′)···O(2) 3.296(3)]. The long

Published on 22 September 2005 on http://pubs.rsc.org | doi:10.1039/B506100H
Downloaded by University of California - Los Angeles on 01 January 2013

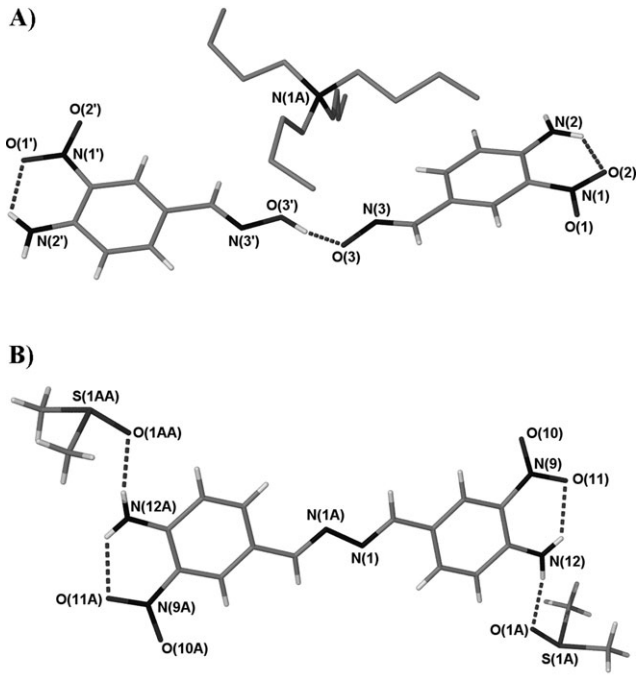

Fig. 2 (A) Compound **7** showing the formation of the oximate–oxime dimer. Selected hydrogen bond length, O(3′)···O(3) 2.509(2) Å. (B) Compound **8**, selected hydrogen bond lengths, N12–H12A···O1A, N···O 2.840(4) Å, H···O 1.98(4) Å. N12–H12A···O11A, N···O 2.657(4) Å, H···O 2.037(3) Å. Hydrogen atoms removed for clarity.

hydrogen bonding interactions are a consequence of the nitro groups on adjacent molecules being in close proximity to one another (the O···O interaction observed at 2.83 Å). This is a surprisingly short distance for an O···O interaction without a bridging hydrogen atom. To date over 100 structures in the crystallographic database show O···O interactions with distances shorter than 2.83 Å. The overall structure is also stabilized due to weak CH···ON interactions. The second oxygen atom on the nitro group is hydrogen bonded to two CH groups in a bifurcated fashion to the adjacent strand. A bifurcated motif of this nature is commonly found in crystal structures and is one of five hydrogen bonding patterns commonly found in weak CH···O hydrogen bonding patterns that involve nitro groups as acceptor moieties as demonstrated by Desiraju.[18] The stability of the complex demonstrates the importance of weak CH hydrogen bonding interactions found in hydrogen bonded polymeric structures.

The strong hydrogen bonding network observed in the X-ray structure is also supported by the solid-state infrared spectrum (Nujol mull). The ν(OH) functionality in the oximate–oxime dimer **7** (N–O···H–O–N) displays a single ν(OH) stretch at 3270 cm^{-1} This is observed at a higher wavenumber than the neutral oxime **4**, (ν(OH) stretch at 3193 cm^{-1}). This bathochromic shift is consistent with strong hydrogen bonding motifs. Which is in good agreement with the short bond lengths obtained from the X-ray diffraction studies, and is commonly found in other oximate–oxime dimers.[19] A strong single absorption band at 1377 cm^{-1} for ν(NO) is observed in the IR spectrum of **7**, which is consistent for aromatic nitrosoamines that have a *trans* geometry, again consistent with the crystal structure.

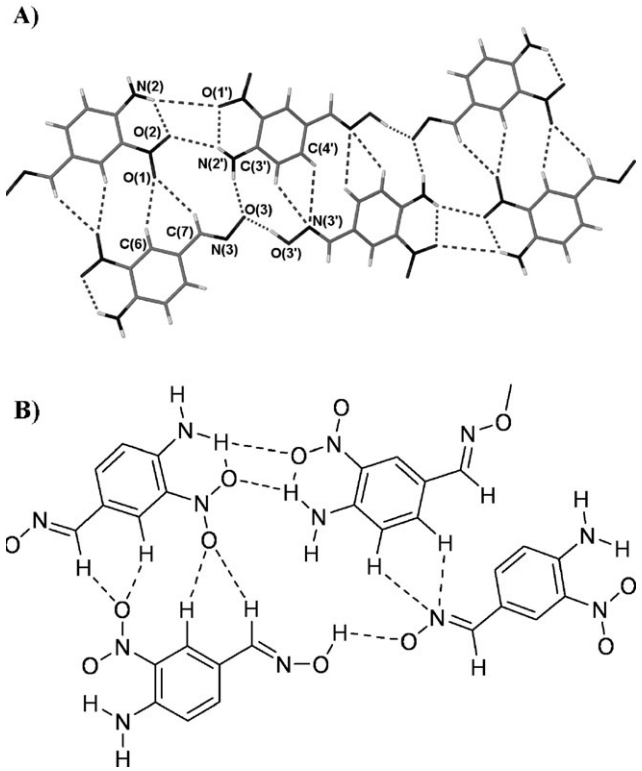

Fig. 3 The crystal packing of (A) **7**, showing the hydrogen bonding polymer of oximate–oxime dimer molecules. Selected bond lengths, N(2′)···O(3) 2.871(3) Å, N(2′)···O(1) 2.658(3) Å and N(2)···O(2) 2.654(3) Å. The tetrabutylammonium counter ion has been removed for clarity. (B) A chemical diagram highlighting the hydrogen bonding in the crystal structure.

X-Ray crystal structure of *E,E* azine (8)

The condensation reaction between hydrazone hydrochloride and the aldehyde **3** in a 1:1 ratio produced the desired hydrazone. It is well known that an azine is the product of two equivalents of a carbonyl group reacting with one equivalent of hydrazone hydrochloride. The characterization of **5** was in good agreement with the proposed structure. However, a DMSO solution yielded X-ray quality crystals that proved to be an azine (compound **8**), Fig. 2b. Glaser *et al*. have carried out an extensive study on *E,E* configured *para*-substituted acetophenone azines.[20–22] They have synthesized a large number of highly polar azine molecules with varying degrees of dipole moment, depending on the functional groups substituted on the benzene core. These highly polar organic molecules show diverse optical and electronic properties that are important in the design of non-linear optic (NOL) materials.[23] The azine functionality in **8** is planar, the torsion angles between N1A–N1–C2–C3 and N1–C2–C3–C4 are 178.8(3)° 176.7(3)°, respectively. The planarity extends across the entire molecule. The amino groups are also in plane with the aromatic ring system. The amines torsion angle is 179.8(4)° (N12–C6–C7–C8). The nitro groups have a slight twist with a torsion angle of 173.3(3)° (C6–C5–N9–O11). Interestingly, virtually all of the compounds studied by Glaser *et al*. show degrees of twisting of the phenyl groups around the azine moiety.[24] However, all of their systems have one substituent in the *para* position, whereas our system has a nitro group *ortho* to the amine functionality. The planarity of the system is a consequence of the intramolecular hydrogen bonding interaction between the amine moiety and the nitro group, 2.037(3) Å.

The bond lengths for N=N, C2=N1, C5–N9 and C6–N12 are 1.411(5), 1.285(4), 1.435(4) and 1.338(4) Å, respectively, and fall in the normal range. However, the C_{ipso}–C_{azine} bond length is 1.453 Å. This seems to be shorter than any bond length previously published in these systems. This can be attributed to the bis-substituted benzene core. The crystal packing of **8** shows classical off-centered face-to-face π–π stacking interactions at a distance of 3.57 Å, which is typical for such interactions.

View Article Online

Conclusion

Two simple chromogenic compounds containing supernucleophile moieties have been attached to a benzene scaffold. Compound **4** can be fully deprotonated and undergoes phosphorylation with DCP and DFP in solution. We are confident that the base does not react with DCP or DFP as a strong and highly hindered phosphazene base was used to confirm phosphorylation. Unfortunately, we were unable to synthesize the salt of the oxime, as a dimer seems to be the more stable species. This was confirmed by X-ray crystal analysis. Currently, there are attempts to prepare fluorescent oxime indicators for CWA detection and these will be published in due course.

Experimental

General techniques

^{1}H and ^{13}C NMR spectra were recorded on a Varian Unity Plus 300 spectrometer in DMSO-d_6. Chemical shifts are reported in parts per million (δ) downfield from tetramethylsilane (0 ppm) as the internal standard and coupling constants (J) are recorded in hertz (Hz). The multiplicities in the ^{1}H NMR spectra are reported as (br) broad, (s) singlet, (d) doublet, (dd) doublet of doublets, (ddd) doublet of doublet of doublets, (t) triplet, (sp) septet and (m) multiplet. All spectra are recorded at ambient temperatures. UV-Vis experiments were performed on a Beckman DU-70 UV-Vis spectrometer. Low and high resolution mass spectra were measured with a Finnigan TSQ70 and VG Analytical ZAB2-E instruments, respectively. IR spectra were recorded on a Perkin-Elmer Paragon 100 Fourier transform IR spectrometer as Nujol mulls, and the peaks of interest were reported in wavenumbers (cm^{-1}) and described as weak (w), medium (m) and strong (s).

General spectroscopic methods

Solutions of **4** and **5** (3×10^{-4} mol dm^{-3}) were prepared in a 1 mol dm^{-1} NaOH–DMSO solution. Aliquots of DFP or DCP (1 μL), were added to a 1 mL UV-Vis cell. The UV-Vis spectrum was recorded after each addition.

4-Acetamido-3-nitrobenzaldehyde (2). 4-Acetamidobenzaldehyde (17 g, 104 mmol) was added slowly to a cold solution (0–5 °C) of fuming nitric acid (44 ml, 940 mmol) and stirred for 2 h. The dark brown solution was then poured into cold water (860 mL). The resulting solid was filtered off and triturated with cold H_2O (430 mL) for a further 1 h. The solid was filtered and then recrystallized from 2-propanol (250 mL), washed with cold 2-propanol (2×50 mL) and dried in the air for 24 h. Yield (11.3 g, 52%), mp 155 °C. ^{1}H NMR: ($CHCl_3$, J/Hz, δ/ppm): 2.37 (s, 3H, CH_3), 8.16 (dd, 1H, $J = 2.0$, 8.7, ArH), 8.73 (d, 1H, $J = 2.0$, ArH), 9.03 (d, 1H, $J = 8.7$, ArH), 9.99 (s, 1H, CHO), 10.62 (s br, 1H, NH), disappears on a D_2O shake. ^{13}C NMR: ($CHCl_3$, δ/ppm): 25.71, 122.17, 127.90, 130.82, 135.44, 135.79, 139.35, 169.17, 188.74. IR (Nujol mull, ν/cm^{-1}): 3340 s (NH), 1710 s (C═O, aldehyde), 1690 s (C═O, amide), 1458, 1377 s (NO_2). CI-MS: $m/z = [M + H]^+$ 209. CI-HRMS: calcd for $C_9H_9N_2O_4$, $[M + H]^+$, 209.056, found, 209.057.

4-Amino-3-nitrobenzaldehyde (3). 4-Acetamido-3-nitrobenzaldehyde (**2**) (5 g, 24 mmol) was added to concentrated HCl (25 mL). The suspension was stirred for 2 h at 75 °C. Cold water (130 mL) was then added to the suspension and stirred for a further 1 h. The resulting solid was filtered and triturated with cold water (130 mL) containing $NaHCO_3$ (5.6 g, 67 mmol) for 1 h. The solid was filtered, washed twice with cold water (50 mL) and crystallized from 2-propanol (250 mL), filtered and washed with cold 2-propanol (2×50 mL). Yield (3.0 g, 75%), mp 191–192 °C. ^{1}H NMR: (DMSO-d_6, J/Hz, δ/ppm): 7.12 (d, 1H, $J = 8.5$, ArH), 7.81 (dd, 1H, $J = 2.0$, 8.9, ArH), 8.18 (s br, 2H, *N*H), disappears on D_2O shake, 8.56 (d, 1H, $J = 2.0$, ArH), 9.76 (s, 1H, CHO). ^{13}C NMR: (DMSO, δ/ppm): 119.89, 124.56, 129.70, 132.45, 132.74, 149.82, 189.63. IR (Nujol mull, ν/cm^{-1}): 3436, 3319 s (NH), 1686 s (C═O, aldehyde), 1463 s (asymmetric), 1407 s (symmetric) (NO_2). CI-MS: $m/z = [M + H]^+$ 167, CI-HRMS: calcd for $C_7H_7N_2O_3$ $[M + H]^+$167.046, found 167.046.

4-Amino-3-nitrobenzaldoxime (4). A suspension of 4-amino-3-nitrobenzaldehyde (**3**) (800 mg, 4.8 mmol) in ethanol (15 mL) was added to a solution of hydroxylamine hydrochloride (670 mg, 9.6 mmol) and sodium hydroxide (386 mg, 9.6 mmol) in water (10 mL) and stirred at room temperature for 7 h. The solution was adjusted to pH 6 by the addition of glacial acetic acid and placed into an ice bath for 1 h. The yellow solid was filtered, washed once with a mixture of glacial acetic acid and water (50 mL, 10 : 1) and recrystallized from ethanol–water. Yield (600 mg, 68%), mp 207 °C. ^{1}H NMR: (DMSO-d_6, J/Hz, δ/ppm): 7.05 (d, 1H, $J = 8.90$, ArH), 7.70 (s br, 3H, NH_2, OH), disappears on D_2O shake, 8.13 (d, 1H, $J = 2.0$, ArH), 11.03 (s, 1H, oxime). ^{13}C NMR: (DMSO, δ/ppm): 119.88, 120.80, 124.43, 129.69, 132.20, 146.20, 146.74. UV-Vis (DMSO, $\lambda = 461$ nm) CI-MS: $m/z = [M + H]^+$ 182. CI-HRMS: calcd for $C_7H_8N_3O_3$ $[M + H]^+$ 182.057, found 182.057.

4-Hydrazonomethyl-2-nitrophenylamine (5). 4-Amino-3-nitrobenzaldehyde (2 g, 12 mmol) was dissolved in 96% ethanol (60 mL), to which hydrazine hydrate (3.52 mmol, 72 mmol) and a catalytic amount of *p*-toluenesulfonic acid (23 mg, 0.12 mmol) were added. The reaction mixture was heated to 70–80 °C for 4 h (during this time period a precipitate formed). The reaction was cooled to 5–10 °C and left to stand at that temperature for a further 1 h. The orange solid was filtered and washed twice with diethyl ether (20 mL) and dried in the air for 24 h. Yield (1.5 g, 75%). ^{1}H NMR: (DMSO-d_6, J/Hz, δ/ppm): 6.59 (s br, 2H, NH_2), disappears on D_2O shake, 7.02 (d, 1H, $J = 8.8$, ArH), 7.52 (s br, 2H, NH), disappears on D_2O shake, 7.67 (m, 2H, ArH), 7.95 (d, 1H, $J = 2.0$, imine). ^{13}C NMR: (DMSO, δ/ppm): 119.72, 121.90, 124.56, 126.76, 132.05, 137.38, 145.79. IR (Nujol mull ν/cm^{-1}): 3399, 3280, 3147 s (NH_2), 1341 s (asymmetric), 1419 s (symmetric) (NO_2). UV-Vis ($CHCl_3$, $\lambda = 425$ nm; MeOH, $\lambda = 432$ nm; DMSO, $\lambda = 461$ nm). CI-MS: $m/z = [M]^+$ 180, $[M + H]^+$ 181 $[2M + H]^+$ 361. CI-HRMS: calcd for $C_7H_7N_2O_3$ $[M + H]^+$ 181.072, found 181.072.

4-Amino-3-nitrobenzaldoxime tetrabutylammonium salt (7). Tetrabutylammonium hydroxide, 1.0 M solution in methanol (21 mL) was added to a methanolic solution (10 mL) of 4-amino-3-nitrobenzaldoxime (**3**) (0.104 g, 0.574 mmol) and stirred for 7 h. During this time a red precipitate was formed, which was filtered and washed with petroleum-ether (5×5 mL) and dried in air for 24 h. Yield (0.247 g, 57.6%). ^{1}H NMR: (DMSO-d_6, J/Hz, δ/ppm): 0.929 (t, 12H, $J = 7.4$, CH_3), 1.30 (q, 8H, $J = 7.4$, CH_2), 1.56 (m, 8H, CH_2) 3.16 (m, 8H, CH_3) 6.87 (d, 2H, $J = 9.0$. ArH), 7.49 (dd, 2H, $J = 2.0$, 9.2, ArH), 7.86 (d, 2H $J = 2.0$, ArH), 7.91 (s, 2H, aldehyde). ^{13}C NMR: (DMSO, δ/ppm): 13.38, 19.11, 22.97, 57.45, 120.78, 122.98, 123.773, 128.66, 130.38, 145.22, 149.89.

X-Ray crystallography for (7). X-Ray experimental for $(C_7H_7N_3O_3)(C_7H_6N_3O_3)^-(C_{16}H_{36}N)^+$: crystals grew as long needles by vapor diffusion of ether into a DMSO solution of the complex. The data crystal had approximate dimensions; $0.50 \times 0.11 \times 0.08$ mm. The data were collected on a Nonius Kappa CCD diffractometer using a graphite monochromator

Published on 22 September 2005 on http://pubs.rsc.org | doi:10.1039/B506100H
Downloaded by University of California - Los Angeles on 01 January 2013

View Article Online

Table 1 Crystallographic data and refinement parameters for compounds **7** and **8**

Compound	**7**	**8**
Chemical formula	$C_{30}H_{49}N_7O_6$	$C_{18}H_{24}N_6O_6S_2$
M	603.76	242.28
Crystal system	Monoclinic	Triclinic
Space group	$C2/c$	$P\bar{1}$
a (Å)	39.7560(6)	6.814(1)
b (Å)	8.4865(2)	8.759(1)
c (Å)	21.6058(4)	11.015(1)
α (°)	90.00	67.536(2)
β (°)	116.6960(10)	76.657(2)
γ (°)	90.00	79.036(2)
U (eÅ^3)	6512.5(2)	587.32(12)
T (K)	153(2)	153(2)
Z	8	1
μ(MoKα) (mm^{-1})	0.087	0.272
Reflections measured	24895	2307
Unique reflections	3527	1596
R_{int}	0.1318	0.0000
R_1 [$I > 2\sigma(I)$]	0.0620	0.0583
wR_2 [$I > 2\sigma(I)$]	0.1010	0.1219
R_1 (all data)	0.1725	0.0956
wR_2 (all data)	0.1261	0.1393

with MoKα radiation ($\lambda = 0.71073$ Å). A total of 418 frames of data were collected using ω-scans with a scan range of 1.1° and a counting time of 76 seconds per frame. The data were collected at 153 K using an Oxford Cryostream low temperature device. Details of crystal data, data collection and structure refinement can be seen in the ESI,‡ and Table 1. Data reduction was performed using DENZO-SMN.[25] The structure was solved by direct methods using SIR97[26] and refined by full-matrix least-squares on $F2$ with anisotropic displacement parameters for the non-H atoms using SHELXL-97.[27] The hydrogen atoms on carbon were calculated in ideal positions with isotropic displacement parameters set to 1.2 × Ueq of the attached atom (1.5 × Ueq for methyl hydrogen atoms). The hydrogen atoms on nitrogen and oxygen were observed in a ΔF map and refined with isotropic displacement parameters. A portion of an *n*-butyl side chain was disordered.

X-Ray crystallography for (8). X-Ray experimental for $C_{14}H_{12}N_6O_4 \cdot 2C_2H_6SO$: crystals grew as small prisms by slow evaporation from DMSO. The data crystal was a prism that had approximate dimensions; 0.20 × 0.15 × 0.06 mm. The data were collected on a Nonius Kappa CCD diffractometer using a graphite monochromator with MoKα radiation ($\lambda = 0.71073$ Å). A total of 324 frames of data were collected using ω-scans with a scan range of 0.7° and a counting time of 214 seconds per frame. The data was collected at 153 K using an Oxford Cryostream low temperature device. Details of crystal data, data collection and structure refinement are listed in Table 1.‡ Data reduction was performed using DENZO-SMN.[25] The structure was solved by direct methods using SIR97[26] and refined by full-matrix least-squares on $F2$ with anisotropic displacement parameters for the non-H atoms using SHELXL-97.[27] The hydrogen atoms on carbon were calculated in ideal positions with isotropic displacement parameters set to 1.2 × Ueq of the attached atom (1.5 × Ueq for methyl hydrogen atoms). The hydrogen atoms on the amino nitrogen, N12, were observed in a ΔF map and refined with isotropic displacement parameters.

Acknowledgements

J. M. thanks the MECD for a "Salvador de Madariaga" sabbatical grant. The authors would also like to thank Intelligent Optical System (IOS) for additional financial support and Dr Steve Cordero for helpful discussions.

References

1 P.-Y. Renard, P. Vayron, F. Taran and C. Mioskowski, *Tetrahedron Lett.*, 1999, **40**, 281.
2 P. Taylor, "Anticholinesterase agents, " in *Goodman and Gilman's The Pharmacological Basis of Therapeutics*, ed. J. G. Hardman and L. E. Limbird, Pergamon Press, New York, 10th edn, 2001, pp. 175–192.
3 Y.-C. Yang, J. A. Baker and R. J. Ward, *Chem. Rev.*, 1992, **92**, 1729.
4 Y.-C. Yang, *Acc. Chem. Res.*, 1999, **32**, 109.
5 S. E. Letant and M. J. Sailer, *Adv. Mater.*, 2000, **12**, 355.
6 S.-W. Zhang and T. Swager, *J. Am. Chem. Soc.*, 2003, **125**, 3420.
7 H. Sohn, S. E. Letant, M. J. Sailer and W. Trogler, *J. Am. Chem. Soc.*, 2000, **122**, 5399.
8 T. Novak, *Anal. Lett.*, 1990, **23**, 169.
9 T. Novak, *Anal. Lett.*, 1991, **24**, 925.
10 T. Novak, *Anal. Lett.*, 1995, **28**, 181.
11 G. Klopman, *Tetrahedron*, 1970, **26**, 4549.
12 V. Z. Shirinian, L. I. Bellenkii and M. M. Krayushkin, *Russ. Chem. Bull.*, 1999, **48**, 2171.
13 A. R. Kiasat, F. Kazemi and F. Khosravian, *Phosphorus, Sulfur Silicon Relat. Elem.*, 2003, **178**, 1377.
14 R. M. Silverstein, G. C. Bassler and T. C. Morrill, *Spectrometric Identification of Organic Compounds*, John Wiley & Sons, New York, 1963.
15 J. K. Maurin, *Acta Crystallogr., Sect. C: Cryst. Struct. Commun.*, 1994, **C50**, 1354.
16 J. K. Maurin, *Acta Crystallogr., Sect. C: Cryst. Struct. Commun.*, 1994, **C50**, 1357.
17 J. K. Maurin, I. C. Paul and D. Y. Curtin, *Acta Crystallogr., Sect. C: Cryst. Struct. Commun.*, 1994, **C50**, 78.
18 S. C. V. Krishnamohan and G. R. Desiraju, *J. Chem. Soc., Perkin Trans. 2*, 1994, 2345.
19 V. V. Ponomarova and K. V. Domasevitch, *Cryst. Eng.*, 2002, **5**, 137.
20 R. Glaser, G. S. Chen, M. Anthamatten and C. L. Barnes, *J. Chem. Soc., Perkin Trans. 2*, 1995, 1449.
21 M. Lewis, C. L. Barnes and R. Glaser, *Can. J. Chem.*, 1998, **76**, 1371.
22 M. Lewis and R. Glaser, *J. Org. Chem.*, 2002, **67**, 1441.
23 M. Petty, C. Bryce and M. R. Bloor, *Introduction to Molecular Electronics*, Oxford University Press, New York, 1995.
24 G. S. Chen, M. Anthamatten, C. L. Barnes and R. Glaser, *J. Org. Chem.*, 1994, **59**, 4336.
25 Z. Otwinowski and W. Minor, *Macromol. Crystallogr., Part A*, 1997, **276**, 307.
26 A. Altomare, M. C. Burla, M. Camalli, G. L. Cascarano, C. Giacovazzo, A. Guagliardi, A. G. G. Moliterni, G. Polidori and R. Spagna, *J. Appl. Crystallogr.*, 1999, **32**, 115.
27 G. M. Sheldrick, *SHELXL-97, Program for refinement of crystal structures*, University of Göttingen, Germany, 1997.

‡ CCDC reference numbers 280696–280697. See http://dx.doi.org/10.1039/b506100h for crystallographic data in CIF or other electronic format.

Published on 22 September 2005 on http://pubs.rsc.org | doi:10.1039/B506100H
Downloaded by University of California - Los Angeles on 01 January 2013